



Molecular Crystals and Liquid Crystals Science and Technology. Section A. Molecular Crystals and Liquid Crystals

Publication details, including instructions for authors and subscription information:

<http://www.tandfonline.com/loi/gmcl19>

High Contrast Twisted Nematic Liquid Crystal Cells for Optical Switching At 1.5 μm

Neil Collings^a, Manuel Bouvier^a, Benno Züger^a & Joachim Grupp^b

^a Institute of Microtechnology, University of Neuchâtel, 2000, Neuchâtel, Switzerland

^b ASULAB S.A., rue des Sors 3, 2074, Marin, Switzerland

Version of record first published: 24 Sep 2006

To cite this article: Neil Collings, Manuel Bouvier, Benno Züger & Joachim Grupp (1998): High Contrast Twisted Nematic Liquid Crystal Cells for Optical Switching At 1.5 μm , Molecular Crystals and Liquid Crystals Science and Technology. Section A. Molecular Crystals and Liquid Crystals, 320:1, 277-285

To link to this article: <http://dx.doi.org/10.1080/10587259808024401>

PLEASE SCROLL DOWN FOR ARTICLE

Full terms and conditions of use: <http://www.tandfonline.com/page/terms-and-conditions>

This article may be used for research, teaching, and private study purposes. Any substantial or systematic reproduction, redistribution, reselling, loan, sub-licensing, systematic supply, or distribution in any form to anyone is expressly forbidden.

The publisher does not give any warranty express or implied or make any representation that the contents will be complete or accurate or up to date. The accuracy of any instructions, formulae, and drug doses should be independently verified with primary sources. The publisher shall not be liable for any loss, actions, claims, proceedings, demand, or costs or damages whatsoever or howsoever caused arising directly or indirectly in connection with or arising out of the use of this material.

High contrast twisted nematic liquid crystal cells for optical switching at 1.5 μm

NEIL COLLINGS^a, MANUEL BOUVIER^a, BENNO ZÜGER^a, AND JOACHIM GRUPP^b

^aInstitute of Microtechnology, University of Neuchâtel, 2000 Neuchâtel, Switzerland;

^bASULAB S.A. rue des Sors 3, 2074 Marin, Switzerland

There is considerable interest in reconfigurable, transparent switches with low loss for both telecom and computing applications. Liquid crystal devices are strong contenders for such applications because they are a tested technology, they can be spatially multiplexed and they can be manufactured at relatively low cost. The main performance criteria of the switch, which should be maintained over a 25 nm bandwidth around 1.55 μm , are: less than 3 dB overall loss per channel, and less than –25 dB crosstalk between channels. These conditions require a liquid crystal cell which rotates the incident polarisation vector by 90° in the off-state, and by 0° in the on-state. In the present work, the cell is first studied by numerical simulation. It is assembled using thick glass plates with low absorption conductive coatings, and peripheral aluminium foil spacers. The simulated results were verified by experiment.

Keywords: twisted nematic liquid crystal cell; liquid crystal modelling

TWISTED NEMATIC CELL: ANALYSIS AND SIMULATION

Gooch and Tarry^[1] have proposed an analytic method to calculate the optical properties of nematic liquid crystal cells. This method considers the liquid crystal as a stack of birefringent slabs each slightly rotated with respect to its neighbour. For a given input polarisation state, the phase shift for each layer and the output polarization state is calculated. This method is very useful for the off-state characteristic of the cell. The minimum thickness of a 90° twist

cell for which the transmission through a parallel polariser/analyser pair is zero, is given by

$$d = \frac{\lambda\sqrt{3}}{2\Delta n}, \quad (1)$$

where λ is the wavelength of the light beam, and Δn is the birefringence of the liquid crystal at that wavelength. The change of thickness with wavelength is also linear.

In order to perform a complete study of a cell, numerical methods are used to calculate the director configuration and the optical properties. These calculations are done with a commercially available software package running on a PC, LCDMaster^[2]. First, the director profile of the liquid crystal must be obtained. The free energy density F is described by ^[3]

$$F = \frac{1}{2}\epsilon\mathbf{E}\cdot\mathbf{E} - \frac{1}{2}\left(k_{11}\text{div}(\mathbf{n}) + k_{22}(\mathbf{n}\cdot\text{rot}(\mathbf{n}) + q_0)^2 + k_{33}|\mathbf{n}\times\text{rot}(\mathbf{n})|^2\right), \quad (2)$$

where \mathbf{E} is the electric field, ϵ is the dielectric tensor, k_{ij} are the liquid crystal elastic constants, \mathbf{n} is the director and q_0 represents the helical pitch.

The Euler-Lagrange differential equation

$$\gamma \frac{\partial n_i}{\partial t} = \frac{d}{dx_j} \left(\frac{\partial F}{\partial n_{i,j}} \right) - \frac{\partial F}{\partial n_i} + \alpha n_i, \quad i=1,2,3 \quad (3)$$

where γ is the viscosity and α a Lagrange multiplier, is solved in time and space for minimum energy with a finite difference method. At the boundaries, a strong anchoring condition is assumed. Once the director profile has been ascertained, two ways of calculating the propagation of light through the liquid crystal media are used: Jones^[4] 2x2 matrix method and Berreman's^[5] 4x4 matrix method. For our calculations, we mainly used the 4x4 matrix method, because it incorporates multiple internal reflection.

Both the analytic and simulation methods require an accurate knowledge of the optical constants of the liquid crystal at the wavelength of interest (1.55 μm). Therefore, we based our study on the liquid crystal ZLI-1565, for which the dispersion of both refractive indices is catalogued in the LCDMaster software. We performed a Cauchy (three constant) extrapolation of the

dispersion curves out to $1.55\ \mu\text{m}$ and found that the ordinary and extraordinary refractive indices were 1.500 and 1.614, respectively. The analytic method gives a minimum at $11.7\ \mu\text{m}$ thickness, with a variation of thickness with wavelength of 7.6. The simulation programme, LCDMaster, has been developed for visible light applications. Therefore, we had to scale the wavelength to the visible region and then scale all other parameters which depend on the spatial dimension. Table 1 shows the actual and scaled parameters. The results of the simulation are shown in Fig. 1.

Parameter	Actual	Scaled
Wavelength	λ	$\lambda/3$
Cell gap	d	$d/3$
Helical pitch	p	$p/3$
Number of layers	N	$N/3$
Rotational viscosity	γ	$\gamma/9$

TABLE 1 List of scaled parameters for simulation in visible region.

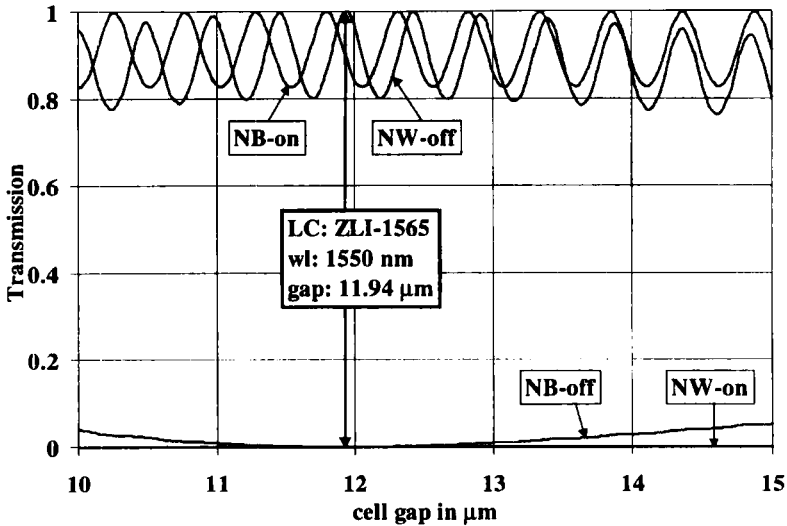


FIGURE 1 The intensity of the transmitted light vs. cell gap. Simulation parameters: LC: ZLI-1565, $\Delta n = 0.114$ at $1.55\ \mu\text{m}$ wavelength, pretilt angle = 2° , $K_{11} = 12.5\ \text{pN}$, $K_{22} = 7.3\ \text{pN}$, $K_{33} = 17.9\ \text{pN}$, $\Delta\epsilon = 10$, 4×4 matrix method.

Both the relaxed (off) and the switched (on) state are shown. When the transmission of the NB off-state equals zero, the cell gap is $11.94\ \mu\text{m}$. The optical properties of a cell including this cell structure were simulated for a cell gap of $11.94\ \mu\text{m}$ with ZLI-1565 and the parameters of Fig. 1. The angular dependence of transmission was calculated using a step of 5° for the azimuth angle (around the optical axis) and 1° for the polar angle (away from the optical axis). In this case, we used the 2×2 matrix method to get the results faster. The results are shown in Figs. 2&3 for the two operating modes, NW and NB, respectively. In the normally white (NW) mode, the polariser and the analyser are aligned with the rubbing directions, and maximal transmission is obtained when no voltage is applied. In the normally black (NB) mode, polariser and analyser are parallel and aligned with one rubbing direction. With no voltage applied, minimal transmission is obtained. It appears that the NB operating mode is less sensitive to angular misalignment than the NW mode. The dark state of the NW mode occurs when the liquid crystal molecules have been aligned by the electric field. Under these conditions, small variations of the incident angle result in an important variation of the effective birefringence and rapid increase of the transmission.

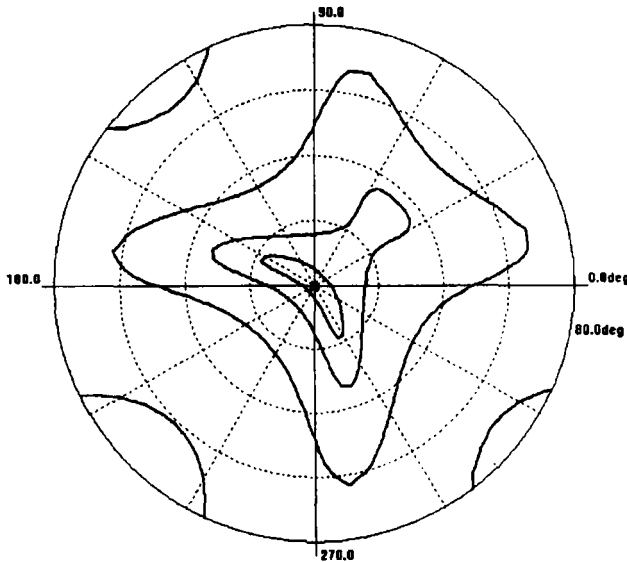


FIGURE 2 Simulated isocontrast contours (30 db, 20 db, 10 db, and 0 db) for the NW configuration. {polar angle: -80° to 80° }

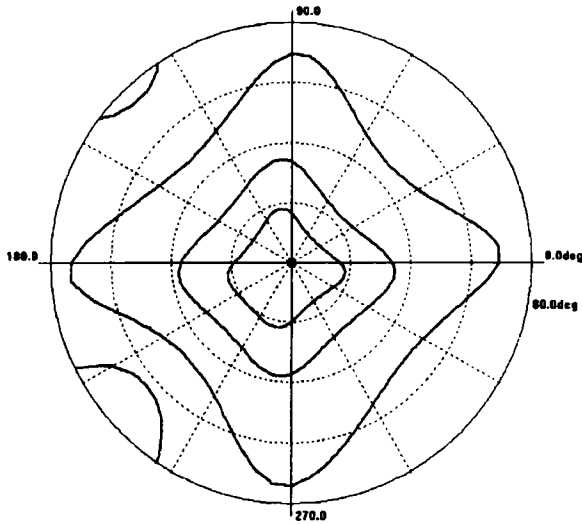


FIGURE 3 Simulated isocontrast contours (30 dB, 20 dB, 10 dB, and 0 dB) for the NB configuration. {polar angle: -80° to 80° }

The study of the liquid crystal cell includes also the glass substrate and other layers such as ITO electrodes, alignment layers and polarisers as shown in Fig. 4.

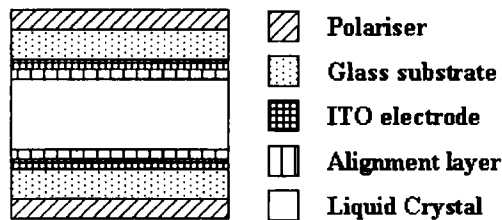


FIGURE 4 Cell structure and parameters. Polariser thickness = $180\ \mu\text{m}$; Glass substrate thickness = $3\ \text{mm}$, $n \approx 1.49$; ITO electrode thickness $\approx 50\ \text{nm}$, $n \approx 1.78$; Alignment layer thickness $\approx 150\ \text{nm}$, $n \approx 1.69$; ZLI-1565 $n_e = 1.614$, $n_o = 1.500$.

TWISTED NEMATIC CELL: FABRICATION AND MEASUREMENTS

Several technological problems appear when constructing a high contrast ratio cell with low losses. Concerning the liquid crystal cell itself, one problem is the

ball or fibre spacers which determine the cell gap. As described by Kimura^[6], the presence of spacers allows the leakage of light in the off-state which reduces the NB contrast ratio. They are also a source of disclinations and misalignment of the liquid crystal, which cause light scattering. Black spacers remedy the first problem, but the light scattering problem remains. A further problem is the non-uniformity of the cell gap due to the statistical spatial distribution of the cell spacers. In order to avoid all these problems, we have used thick glass (3 mm) whose rigidity permits us to remove the spacers from the active zone. Four thin aluminium films placed at the corners of the glass plates have been used as spacers.

Another aspect to consider is the transmittivity of each layer, such as the glass substrate, ITO layer, and the alignment layer. Fig. 5 shows the measurements of the transmittivity for different types of ITO layers.

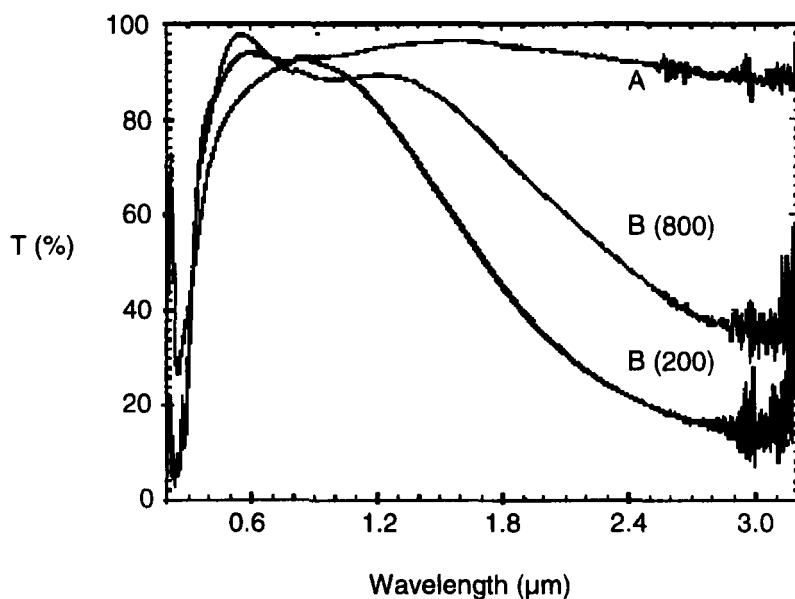


FIGURE 5 Transmission of thick and thin commercial ITO (B(200) and B(800)) and Ion-Assisted Deposited ITO (A)

The commercial layers (Baltracon from BALZERS) have a strong decay of the transmittivity in the infrared due to free carrier absorption. Therefore, we made ITO layers with an Ion Assisted Deposition (IAD) technique, which reduces free carrier absorption and, consequently, increases the transmission at the desired wavelength. Finally, the quality of the polarisers limits the maximal contrast ratio performance. For the measurements, Glan-Thompson polarisers

with a contrast ratio over 50 dB were used, whereas for the simulations, film polarisers (HR 8) with a maximum contrast ratio of 39 dB had been used. The experimental characterisation of the cells was performed with a multimode diode laser whose output consisted of a series of lines between 1.52 μm and 1.54 μm wavelength and an AlGaAs detector. The measurements were first performed at different cell gaps using wedged cells, and, afterwards, flat cells based on the results were constructed for assembly in a complete switch. For the wedged cells, we used different spacer thicknesses at the two sides giving a linearly increasing cell gap ranging from 8 to 18 μm over a length of 26 mm. In Fig. 6(a), numerical simulation and measurements of the wedged cell are compared. The peak contrast ratio of the measurements is shifted to smaller gaps with respect to the simulation.

According to the results obtained from the wedged cells, flat cells with a cell gap close to the optimum were constructed using 12 μm thick aluminium foil, and tested. Table 2 shows the results obtained in these cells. Figs. 6(b) and (c) show the angular behaviour for both operation modes. In accordance with the simulation, NW is more sensitive to angular variations, while NB is more tolerant.

Configuration	AE2 [dB]	DG2 [dB]	BH2 [dB]
Para, NB	46.7	48.9	47.3
Perp, NB	45.4	46.7	47.6
Para, NW	>40 (48.8)	>41 (48.2)	>41 (51.2)
Perp, NW	>40 (48.3)	>43 (52.4)	>40 (49.5)

TABLE 2 The contrast ratios of three flat cells measured in four configurations, NB and NW with initial polarisation parallel and perpendicular to the incident director. Figures in brackets refer to high driving voltage (20 V peak-to-peak).

CONCLUSION

We have constructed TN cells with high contrast in both normally white and normally black operating modes for a switch in the near infrared region (1.55 μm). The characteristics of the cells were first obtained by computer simulation, and later verified by experiments. It has been demonstrated that analytical methods and numerical simulations are useful tools for predicting cell characteristics.

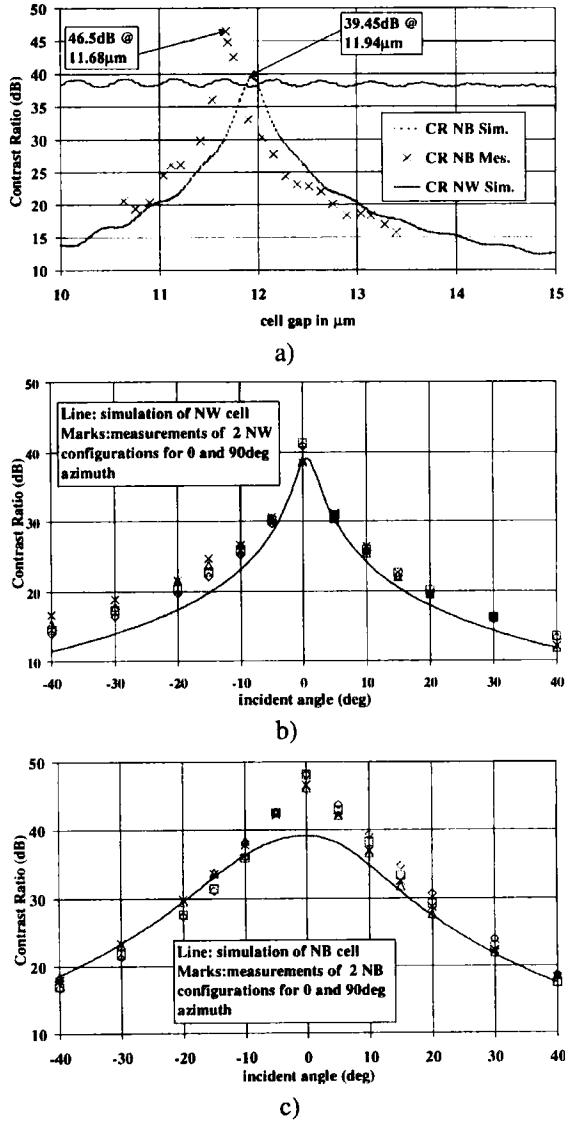


FIGURE 6 (a) Comparison of measured (NB) and simulated(NB, NW) contrast ratio with ZLI-1565 (b) Contrast ratio vs. incident angle for NW and 0° and 90° azimuth (c) Contrast ratio vs. incident angle for NB and 0° and 90° azimuth.

The analytical method predicts an optimum cell gap of $11.77 \mu\text{m}$ @ $\lambda = 1.55 \mu\text{m}$ and $11.62 \mu\text{m}$ @ $\lambda = 1.53 \mu\text{m}$. The simulation predicts an optimum cell gap of $11.94 \mu\text{m}$ @ $\lambda = 1.55 \mu\text{m}$. The measurements on the wedged cell give an optimum gap of $11.7 \mu\text{m}$ @ $\lambda = 1.53 \mu\text{m}$. The experimental measurement of the optimum gap is subject to error because it is not an in situ measurement. Therefore, the agreement between simulation and experiment is reasonable. Moreover, the agreement is good with regard to the angular variation of contrast ratio, where the analytic method is more complex and we have to rely on simulation.

The future work is directed towards a multichannel version of the solid optics switch presented by Fujii^[7], using a 24-pixel version of the flat cell.

REFERENCES

- [1] C.H. Gooch and H.A. Tarry, *J. Phys. D: Appl. Phys.* **8**, 1575-1584 (1975)
- [2] LCDMaster from Shintech Inc., 90 Ogou-oku, Tabushe-cho, Kumage-gun Yamaguchi, 742-15 Japan
- [3] F.C. Frank, *Discuss. Faraday Soc.*, **25**, 19-28 (1958)
- [4] R.C. Jones, *J. Opt. Soc. Am.*, **38**, 671-685 (1948)
- [5] D.W. Berreman, *J. Opt. Soc. Am.*, **68**, 1374-1380 (1973)
- [6] K. Kimura et al., *Opt. Lett.* **17**, 1647-1649 (1992).
- [7] Y. Fujii, *IEEE Phot. Tech. Lett.* **5**, 715-718 (1993).